ELSEVIER

European Journal of Cardio-thoracic Surgery 31 (2007) 915–921

EUROPEAN JOURNAL OF CARDIO-THORACIC SURGERY

www.elsevier.com/locate/ejcts

Analysis of the fiber architecture of the heart by quantitative polarized light microscopy. Accuracy, limitations and contribution to the study of the fiber architecture of the ventricles during fetal and neonatal life☆

Pierre-Simon Jouk [a,b,*], Ayman Mourad [c,d], Vuk Milisic [d], Gabrielle Michalowicz [a,b], Annie Raoult [c,e], Denis Caillerie [f], Yves Usson [b]

[a] Department of Genetics, Grenoble Teaching Hospital, BP 217, 38043 Grenoble Cedex 09, France
[b] Equipe Reconnaissance des Formes et Microscopie Quantitative—Laboratoire TIMC, UMR 5525 CNRS, Grenoble, France
[c] Laboratoire Modélisation et Calculs, IMAG, Grenoble, France
[d] Bioengineering Institute, Private Bag 92019, Auckland, New Zealand
[e] MAP5, Université Paris 5-René Descartes, 45 rue des Saints-Pères, 75270 Paris, France
[f] Laboratoire Sols, Solides, Structures, Grenoble, France

Received 27 July 2006; received in revised form 4 December 2006; accepted 5 December 2006; Available online 12 March 2007

Abstract

Objective: To address the advantages and drawbacks of quantitative polarized light microscopy for the study of myocardial cell orientation and to identify its contribution in the field. **Methods:** Quantitative polarized light microscopy allows to measure the orientation of myocardial fibers into the ventricular mass. For each pixel of a horizontal section, this orientation is the mean value of the directions of all myosin filaments contained in the thickness of the section for each pixel of the section and is accounted for by two angles, the azimuth angle, which is the angle of the fiber in the plane of the section, and the elevation angle, which measures the way the fiber escapes from the section. The azimuth is accurately measured, and its range of definition is complete from 0° to 180°. The elevation angle can be defined only in the range 0° to 90°. It is accurately measured between 20° and 70°. From 0° to 20°, there is a systematic bias raising the measured values, and from 70° to 90°, the angle is not accurately measured. **Results:** With this method, we validated Streeter's conjecture concerning the architecture of the left ventricle. We formulated a pretzel conjecture about the fiber architecture of the whole ventricular mass during fetal period. In our model, elaborated by visual analysis of registered maps of orientation, the fibers run like geodesics on a nested set of 'pretzels'. Next, the validity of the helical ventricular myocardial band model of Torrent-Guasp has been examined. It appears that the band model does not account for the patterns observed in our data during the fetal period. However, after the major events of postnatal cardiovascular adaptation, our data can neither discard nor confirm Torrent-Guasp's model. **Conclusions:** Present limitations of quantitative polarized light analysis can neither confirm nor discard the existing models of fiber orientation in the whole ventricular mass after the neonatal period. However, the problems of mathematical and experimental validation of these two models have been posed in a rigorous manner. Non-ambiguous fiber tracking and demonstration of these models will require significant improvement of the definition range of the elevation angle that should be extended to 180°.

Keywords: Polarized light microscopy; Myocardium; Structure

1. Introduction

The fiber architecture of the heart is still actually debated. This is essentially due to the technical difficulties for the extraction of the information about orientation in space of the myocardial cells. A lot of techniques have been used over the years. The first one was dissection, and we have to acknowledge the works of Krehl [1], Mall [2], Robb and Robb [3], Rushmer et al. [4], Lev and Simkins [5], Grant [6], Torrent-Guasp [7], Fernandez-Teran and Hurle [8], Greenbaum et al. [9], and Sanchez-Quintana et al. [10]. Others have used classical histological techniques, Hort [11], Fox and Hutchins [12] and finally Streeter [13] with a great effort toward quantification. Recently, new imaging techniques using resonance diffusion tensor imaging [14] have been introduced. In the same time, new microscopic techniques using polarized light analysis have been thoroughly developed [15]. All these techniques are confronted to the same problem that is essentially the artifactual nature of the fiber

☆ Presented at the meeting, Cardiodynamics: Ventricular Wall Structure and Cardiac Function, Zurich, Switzerland, November 4–5, 2005.

* Corresponding author. Tel.: +33 4 76 76 54 82; fax: +33 4 76 76 88 50.
E-mail address: psjouk@chu-grenoble.fr (P.-S. Jouk).

1010-7940/$ – see front matter
doi:10.1016/j.ejcts.2006.12.040

entity. There is no anatomic structure that corresponds with a 'fiber' such as one can isolate from the skeletal muscle. The myocardial body consists of aggregates of myocytes which are three-dimensionally netted. In this network, each technique tries to identify the long axis of the aggregated myocytes, a preferential pathway minimizing the variation of the orientation along successive cells and call it a 'fiber'. For this goal, each technique has advantages and drawbacks that can be summarized as follows. With dissection techniques, the reproducibility is uncertain especially in the area where the network of fibers is complex. With classical histological techniques, for instance, it is only possible to study a very small part of the whole ventricular mass. Consequently, inference of these local data to the organ remains difficult. With resonance magnetic imaging, the issue is presently the low spatial resolution as a few voxels only can be studied across the thickness of the ventricular walls. The description of the fiber architecture of the ventricular mass in normal and pathological hearts is a complex issue that will probably be solved by using several of the former techniques in association. The main goal of this paper is to address both the present accuracy and limitations of quantitative polarized light microscopy. First, we will give a didactic overview of this technique, and second, we will explain what its contribution in the field has already been. Polarized light microscopy already helped to (i) validate Streeter's conjecture about the fiber architecture of the left ventricle; (ii) elaborate a conjecture for the whole ventricular mass; and (iii) test the validity of some other models. The modifications in the fiber patterns during perinatal adaptation will highlight another fundamental point: fiber orientation is essentially an adaptive process and when comparing data and checking models, it is necessary to take into consideration the developmental stage under study. Finally, an additional aim of this paper is to help researchers to choose the appropriate methods for their own studies.

2. Materials and methods

All the studies reported here have been performed on routine histological sections of hearts of human fetus and infants embedded in methyl methacrylate (MMA). All tissues were obtained in compliance with French legal and ethical guidelines.

Quantitative polarized light microscopy: light is an electromagnetic wave, it vibrates perpendicular to the direction along which it propagates. Usually, light is composed of waves whose vibration axes are randomly distributed. However, after reflection or transmission across a polarizing device, the vibration axes of the rays become parallel, light is polarized. We designed an optical bench to study fiber orientation with polarized light. It is made of the following items: a white light source, a first linear polarizing filter that is the polarizer, a stage to hold the specimen, another linear polarizing filter that is the analyzer whose vibration axis is perpendicular to that of the polarizer and finally a CCD camera that measures the amount of transmitted light. In this setting, polarized light is not modified when an isotropic specimen or a birefringent sample with a main axis parallel to the vibration axis is placed in the optical path. In such a case, light vibrates perpendicular to the analyzer and no light comes out of it. On the contrary, when a birefringent sample is rotated in the polarized light, it interferes with the light vibration axis and some light is transmitted across the analyzer. Thus, the amount of transmitted light is a function of the birefringence of the sample, and this birefringence is a function of the physico-chemical characteristics of the sample and its orientation with respect to the light. This property has been known for long for crystals, and is also true for fetal myocardial tissue that behaves like a quasi-crystal. This is illustrated with a papillary muscle of the mitral valve (Fig. 1). Caveat: The myocardial birefringence is due to different molecules, the crystalline birefringence of myosin that is uniaxial positive and the structural or form birefringence of collagen. This second type of birefringence is highly variable according to the kind of collagen under examination and must be eliminated as much as possible. This is done by embedding the samples in MMA that has the same refraction index than collagen. Therefore, myocardium embedded in MMA behaves like a quasi-crystal and quantitative polarized light can be used for characterization of its properties. Note that the purposes of mineralogists and biologists are completely opposite, which means that we have to design our own experimental device. The mineralogist wants to identify the sample and for that purpose breaks it in very small pieces dispersed in the microscopical field. From the whole of the information such gathered, the mineralogist determines the uniaxial or biaxial nature of the birefringence, the value of maximum birefringence and by referring to an atlas is able to name his sample. The biologist already knows the birefringence characteristics of his sample and wants to use these properties of modulation of the amount of transmitted light to obtain some information about the myosin orientation. For that biological purpose it is necessary to insert a section of the heart embedded in MMA on the microscopical stage and to vary the conditions of illumination with a beam of linearly polarized light (Fig. 1). For each condition of illumination and for each pixel of the CCD camera, there will be a value of transmitted light. From an appropriate numerical treatment based on optical laws of these data, we are able to infer the mean spatial orientation of the myosin filaments for each pixel of the section. This orientation in space can be described by means of two angles: the azimuth angle and the elevation angle. The azimuth is the angle between the east–west axis of the stage and the projection of the fiber direction on the stage plane. The elevation angle corresponds to the obliquity of the fiber with respect to the plane of the section, which is the way the fiber escapes from the section plane. In order to obtain the values of the azimuth and elevation angles, it is necessary to grab 12 pictures corresponding to a properly selected combination of the crossed polarizer and analyzer orientations [15,19]. The results are given in the form of selected maps of the elevation and azimuth angles of the myocardial fibers (Fig. 2).

2.1. Accuracy and limitations of the method

The method highly relies on the nature of the molecule whose orientation is well defined, namely the myosin molecule. Myosin is one of the major contractile proteins, and is aligned with cells and fibers. This is the basis of our method design and robustness. Next, the polarized light

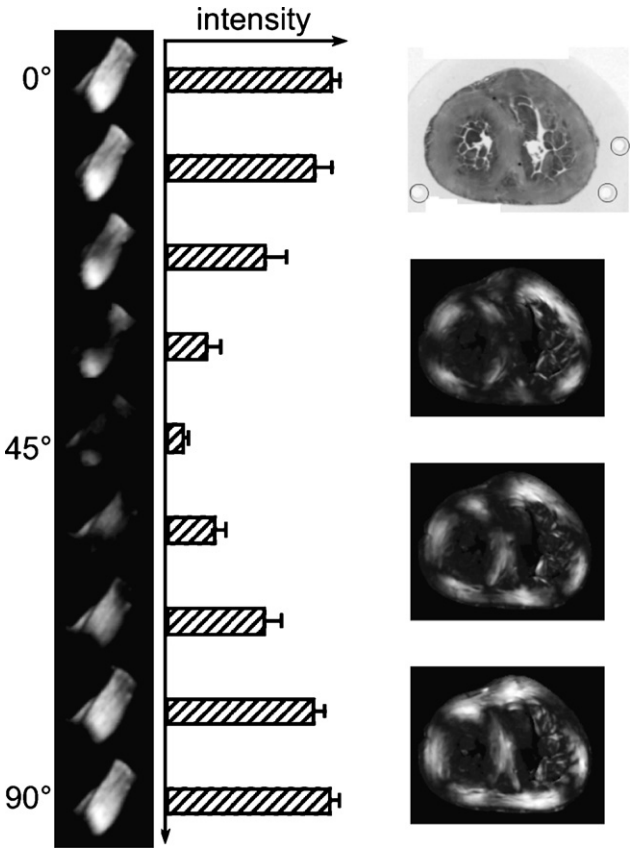

Fig. 1. Variation of transmitted light according to the angle between the vibration axis of the polarized light and the fiber axis. Left column: Section of a papillary muscle where fibers are mostly parallel. It lays on the stage with an angle of 45° with reference to the east–west axis of the stage, the 0° line. From top to bottom: Images of the papillary muscle collected while rotating the crossed polarizer and analyzer. The crossed polarizing filters are initially in a position with the axis of the polarizer at 0°, then they are progressively rotated and the amount of transmitted light is measured. Initially, when the angle between the fibers and the vibration axis is 45°, the intensity of transmitted light is maximal. Then it decreases progressively to become extinct when fibers and polarizer are parallel (the only transmitted light occurs at the level of some divergent fibers). Then, the intensity increases again until fibers and polarizers are again at 45° from each other. Middle column: Plot of transmitted light measured at increasing steps of 11.25°. This curve matches the theoretical curve of a uniaxial positive crystal with a goodness of fit: $r^2 = 0.99$. Right column: Top, 500 μm thick section of the heart embedded in MMA. The fiducial markers are drilled previously to sectioning; they are used for subsequent registration of the sections. Below: Three images of the same section in polarized light for angles of the crossed polar varying from 0° to 45° by steps of 22.5°. We observe that on the upper picture, the axis of the polarizer is 0°, and the fibers at 45° modulo 90° are highlighted. On the lowest picture, the axis of the polarizer is 45°, and the fibers at 0° modulo 90° are highlighted. Mid picture: The polarizer is in the intermediate position (22°5), intermediate fibers are highlighted. Moreover, fibers that lie in the plane of the section are brighter than fibers that are perpendicular the section, for example in the subendocardial area.

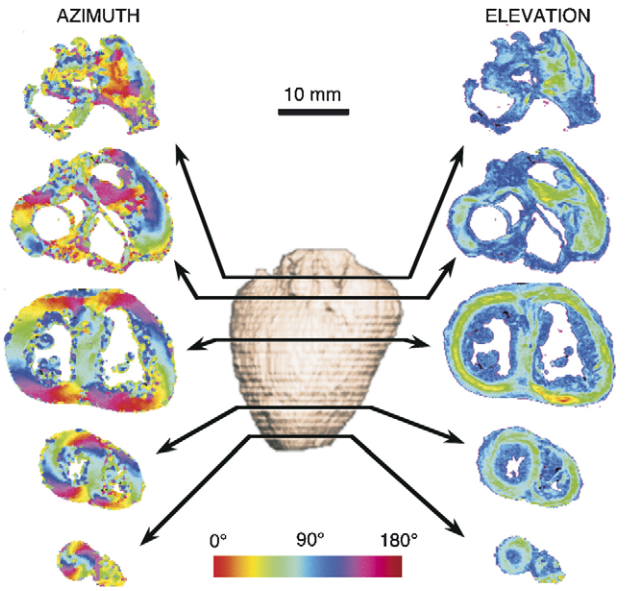

Fig. 2. Maps of azimuth and elevation angles. The whole ventricular mass is serially sectioned. A few examples of azimuth and elevation maps are shown. The azimuth is coded in false colors from 0° to 180°. For example, there are red fibers at the diaphragmatic face of the heart with a 0° azimuth angle, and blue fibers in the interventricular septum and lateral wall of the ventricles with a 90° azimuth angle. On the equatorial azimuth map (third row), the values of the azimuth angle vary in sympathy with the curvature of the left ventricular wall, while turning around the left ventricle azimuth is rotating with a smooth progression from one color to the other. This means that the fibers are circumferential. Toward the apex, a spiral anticlockwise arrangement is visible, while the basal maps show a spiral arrangement with an inverse sense of rotation. The elevation angle is coded in false colors from 0° to 90°.

method integrates the orientation information within each pixel and gives a mean value of the orientation of all the myosin filaments contained in the thickness of the section for each pixel. Moreover, resolution is high: in most cases, we choose the size of the voxel to be 100 μm × 100 μm × 500 μm. The width of the voxel can vary according to the degree of enlargement of the objective lens that runs from 10 μm × 10 μm to 500 μm × 500 μm, while the thickness coincides with the 500 μm section thickness. Finally, the range of definition of the azimuth is 180° (π)—thus, it is complete—with a ±1° accuracy. Let us now list the limitations that we are facing: the definition range of the elevation angle is restricted to 90° (π/2). Thus, the angle of elevation is not completely defined. The accuracy of the measurement is 1°, as previously, but only between 20° and 70°. Between 70° and 90°, the very low amount of transmitted light does not make it possible to resolve the angle. Between 0° and 20°, there is a systematic bias of the measurement of the elevation angle. This is a consequence of the usual dispersion of fiber orientation around the mean orientation and of the incomplete range of definition of the elevation angle. When the mean elevation comes close to 0°, the negative values are folded up into the positive domain and consequently the mean elevation angle remains bigger than its actual value. Another limitation of our technique is that we have to disregard the structural birefringence of collagen. This is possible during the fetal period and the first 3 months of postnatal life but not at later stages. This is probably a consequence of the collagen increase and the diversification of collagen molecules. Three months after birth, the birefringence of myocardium is no longer uniaxial but biaxial. This feature should not be seen as a definitive impossibility for the extraction of orientation information, but it increases the complexity of the task. Taking it into account would require progress in instrumentation. Our technique cannot be used either in case of notable uneven distribution of collagen, for example when there is subendocardial fibrosis. Finally, there are also limitations due to the size of the myocardium sample. The present thickness of the sections we analyze is 500 μm which happens to be optimal

for image analysis. We were able to reduce the section thickness to 300 μm, but this resulted in an increase of the artifacts due to the thickness variation along the section: a 20 μm discrepancy can be observed between the thicker point and the thinner point. In addition, reducing the section thickness decreases the signal-to-noise ratio. Therefore, it is difficult to study ventricles that are smaller than 1.5 cm in length, because in such a case, geometrical variation in curvature of the ventricular wall inside the section is no longer negligible. As for the maximal size of the ventricles, it is limited by the embedding and sectioning processes. Actually, acrylic polymerization is exothermic and the induced overheating for large samples can denature proteins. It was not possible to embed hearts larger than 10 cm. This makes it difficult to obtain larger sections with constant thickness. Each studied section requires about 1 h of technical work, and the mean number of sections studied for one heart varies between 20 and 70. Although time consuming, the method provides serially related maps of orientation theoretically enabling fiber tracking.

2.2. Fiber tracking

The chosen algorithm is classical for integration of ordinary differential equations and is based on a second-order Runge–Kutta method [16]. For a field of vectors, finding a curve that is tangent at each point to the given vectors is a classical problem. The algorithm we use is a basic algorithm for the integration of ordinary differential equations and is based on a second-order Runge–Kutta method [16]. At this point of the description, we need to clarify the concept of fiber. Fibers tracked by our method of polarized light microscopy are statistical entities. As far as we know, in normal myocardium, sarcomeres and myosin filaments are aligned along the main direction of the myocardial cell. Therefore, there must be good correlation between the myosin path that we determine and fiber paths observed by anatomists. Indeed, these fiber paths observed by anatomists are bundles of myocardial cells longitudinally connected one to another by intercalary discs and wrapped by a collagen scaffold. Incidentally, this is the place where to mention a limitation of our experimental device which actually lies outside of the scope of the present paper: as we cannot see the collagen, we are unable to study the relationships between fibers and the collagen scaffolding'. A final limitation related to the drawbacks of the experimental device we already mentioned is some ambiguity in fiber tracking. Indeed, the 180° azimuth range and the 90° elevation range define only a quarter of a sphere. The only present solution is to perform fiber tracking seed by seed, each track requiring a visual confirmation for anatomical pertinence. To conclude, we remind that fiber tracking can be performed only for fibers with an elevation angle between 20° and 70°.

3. Results

3.1. Validation of Streeter's conjecture concerning the fiber architecture of the left ventricle

Streeter's conjecture was based on a very limited sample of the left ventricular wall [17,18]. Our data concern the whole ventricular mass and allow to test Streeter's conjecture on a larger scale. Streeter's conjecture was stated by himself in this very condensed sentence 'Myocardial fibers run like geodesics on a nested set of toroidal bodies of revolution'. This mathematical language remains very obscure to the anatomist and to the cardiologist. Let us clarify it a bit: first, the nature of the surface on which the fibers run has to be defined; second, the definition and properties of geodesics have to be reminded; third, the form of the surfaces 'toroidal bodies of revolution' must be explained. First, what are these surfaces? For the mind visualization of such a surface, you have to choose first a fiber and then to select among the neighboring fibers the one that has the closest orientation, and to reiterate the process. Actually, the surfaces are defined by the fibers themselves, as in a ball of wool. Second, each fiber runs like a geodesic that is the shortest path between two points of the surface. Let us give some basic examples of geodesic curves: when the surface is a plane the geodesic curve is the straight line joining the two points, when the surface is a sphere, the geodesic between two points is the arc of the circle passing by the two points and whose center coincides with the center of the sphere. For cylinders, geodesics are straight lines, planar circles, and helices. This common definition is only locally true; mathematically speaking, a geodesic can also be defined as a curve whose principal normal coincides with the vector perpendicular to the surface. Third, the surfaces are toroidal and nested. That means that each fiber runs on a tore. Moreover, each surface is entirely covered by the set of fibers (Fig. 3) and all surfaces are nested. The anatomical validation of Streeter's conjecture relies on a property of geodesics stated by Alexis-Claude Clairaut (1713–1765). Geodesics running on surfaces with symmetry of revolution

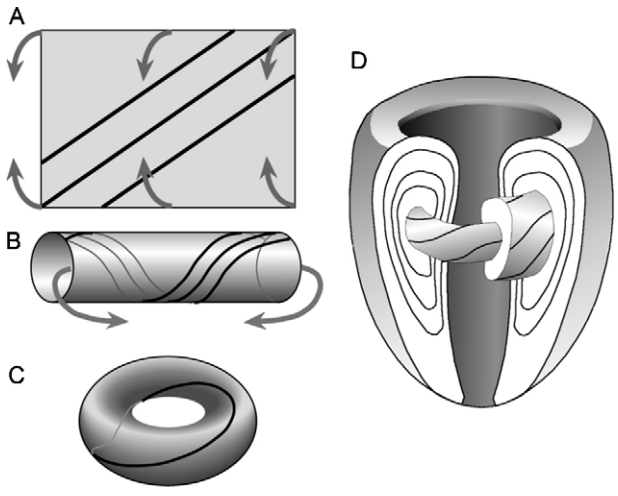

Fig. 3. Illustration of Streeter's conjecture: 'Myocardial fibers run like geodesics on a nested set of toroidal bodies of revolution'. Construction of a torus from a sheet of paper: (A) first step, take a sheet of paper and draw three parallel lines. These lines are geodesics of the plane surface; (B) second step, roll the sheet, superior border against inferior border, you obtain an open cylinder, the drawn lines remain geodesics of the cylinder; (C) third step, bend the cylinder until the left end reaches the right end, you get a torus on which the lines are still geodesics. It looks like a swimming belly. (D) Streeter's conjecture where the elongated tori are nested like Russian dolls. On the section of the left ventricular walls are represented the lines of section of the outer torus and the innermost torus is represented emerging from the section.

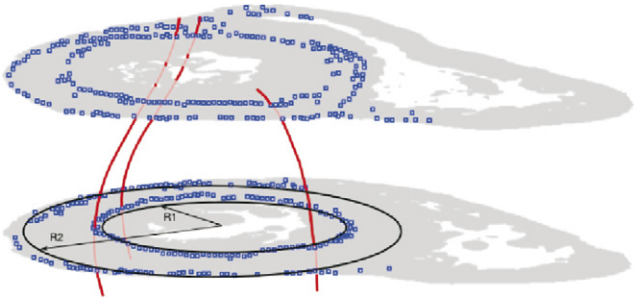

Fig. 4. Anatomical and experimental validations of Streeter's conjecture. Two coronal sections of one fetal heart are represented. For a given value of the Clairaut constant, on each section, the set of points with this value is distributed along two concentric circles. Three fiber tracks have been propagated from three seeds. Trajectories running from a seed located on a circle with a selected Clairaut constant intersect the subsequent sections at points which are also isovalues of the same Clairaut constant. Thus, each value of the Clairaut constant defines a torus, whose intersections with the coronal sections are represented by the circles. The tracked fibers run on the surface of this torus.

have on each point an equal value of the Clairaut constant $r \cos \theta$, where r is the distance of the considered point to the axis of revolution and θ the angle that the curve makes with the parallel that intersects it. Therefore, three properties must be verified: (i) on saggital sections, isovalues of the Clairaut constant must be symmetrically distributed along closed curves; (ii) isovalues of Clairaut constant on coronal sections must be on concentric circles; and (iii) fibers running from a coronal section to another must join isovalues of the Clairaut constant. The Clairaut value happens to be easily computed from the experimental orientation data. This allowed us to check that the three properties were actually true [17,18]. A representation of the results is given in Fig. 4. This is an experimental demonstration of Streeter's conjecture during fetal life.

3.2. Elaboration of a pretzel conjecture about the fiber architecture of the whole ventricular mass during fetal period

This model was elaborated by visual analysis of orientation maps [19]; consequently, it must be viewed only as a conjecture. It consists in an extension of Streeter's model of the left ventricle to the whole ventricular mass. In this model, fibers run also in the right ventricle like geodesics on a nested set of toroidal bodies that are no more of revolution (Fig. 5). Mathematical and experimental validations of this conjecture are still to be done. Since no symmetry can be assumed, we cannot make use of such an easy criterion as the Clairaut property. Theoretical criteria based on the properties of the binormal to a geodesic curve proved to be too sensitive to have a numerically tractable formulation.

4. Checking the validity of other models

Presently, there is no experimentally and quantitatively demonstrated model of the fiber architecture of the whole ventricular mass, but we will discuss the compatibility of our data with the presently most discussed model: The helical ventricular myocardial band of Torrent-Guasp. During fetal period, there is clearly no compatibility of our data with Torrent-Guasp's model. In this model, while unrolling the right ventricular free wall, it is possible to observe a continuity with the left ventricular free wall, diaphragmatic part then lateral wall, this is the basal loop. At this stage, the unrolling of the right ventricular free wall conducts directly

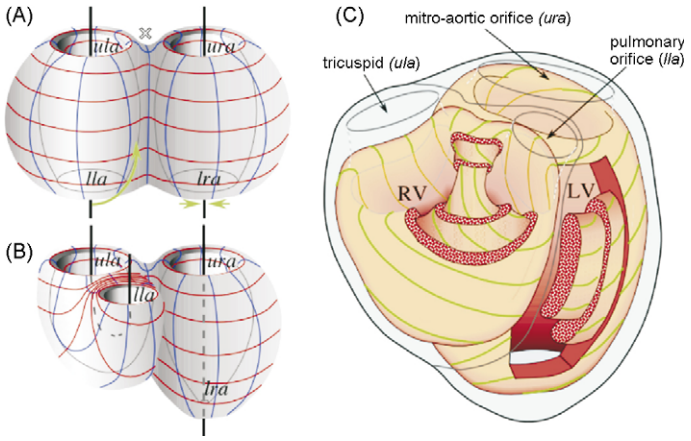

Fig. 5. Schematic description of the pretzel model about the fiber architecture of the whole ventricular mass. (A) To comprehend our model, it is useful to start from two joined tori that form a pretzel. A lattice is drawn on the surface to grasp further deformations. In blue the meridians, in red the parallels of this surface of revolution. *lla*: lower left aperture; lra: lower right aperture; *ula*: upper left aperture; *ura*: upper right aperture. (B) The torus on the left is bent in such a way that the lower aperture comes up close to the upper aperture. This conformation roughly mimics the right ventricle shape. The lower aperture of the right torus constricts to a point where no lumen is left. This conformation roughly mimics the left ventricle shape as explained in (C). Part (C) shows how such topological pretzels would nest into the ventricular mass as seen in front view. In green, representation of geodesics on the nested pretzels. In the left ventricle, we retrieve the classical Streeter's model. Wedges have been cut out in the left ventricular wall to show the nested tori. The organization shown in the right ventricle is our original contribution to the description of the fiber organization in the whole ventricular mass. Considering the pretzel model, the upper left aperture would correspond to the tricuspid orifice and the lower left aperture to the pulmonary orifice. Between these two apertures is the supraventricular crest. In this representation, it is given by the narrow part of the nested bent tori. While the wide part of the bent tori corresponds to the septal and lateral walls of the right ventricle. On the supraventricular crest, the most external torus walls have been cut out, in order to show schematically three nested tori. The innermost part shows the continuity of the torus walls inside the supraventricular crest.

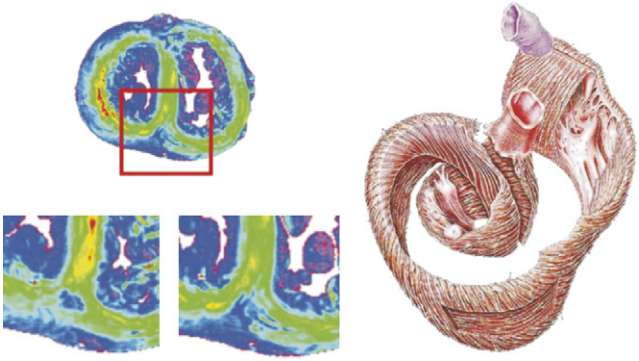

Fig. 6. (A) Elevation map of a coronal section of a fetal heart (37 weeks gestation) at the atrioventricular papillary muscles level. The left ventricle is on the left. The red square highlights the inferior part of the ventricular septum shown below at a higher magnification. In the same heart, two separate patterns of fibers can be observed according to the sectioning level in this area. On the right, the predominant pattern, the medial circumferential fibers (yellow green) of the left and right ventricles converge into the circumferential medial part of the interventricular septum. On the left, the less frequent pattern, where the circumferential fibers of the left and right ventricles are either in continuity or converging toward the interventricular septum. (B) Adaptation of Torrent-Guasp helical myocardial band for comparison (by courtesy of Pr Paul Lunkenheimer and IOS Press). This model does not account for the patterns observed in our data.

onto the interventricular septum; this is clearly shown in Fig. 6 featuring an elevation map of a coronal section at the basal loop level. Thus, there is no basal loop in the fetal period and no compatibility for this period with Torrent-Guasp's model. But after birth, major adaptations occur; this is illustrated in Fig. 7. These postnatal adaptations concern not only the relative volume of the ventricular walls; they also concern the fiber architecture. This is well seen in Fig. 8 where we chose two sections that highlight hypothetical

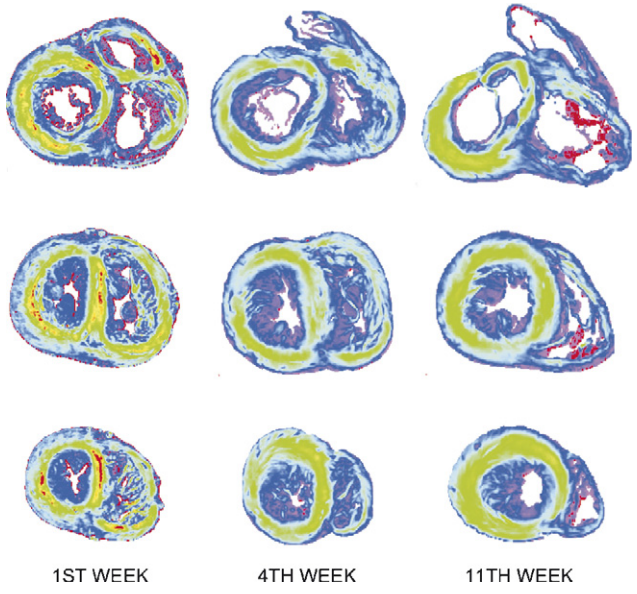

Fig. 7. Elevation maps of basal, equatorial and apical coronal sections of three hearts of term infants dead at birth, at 3 weeks postnatal life and 10 weeks postnatal life for extracardiac reasons. They are shown with different scales, so that they are of similar size. This allows us to highlight the relative changes of the thickness between the left and the right ventricular wall. Analysis of the inferior part of the IVS shows a massive rearrangement of the fiber architecture.

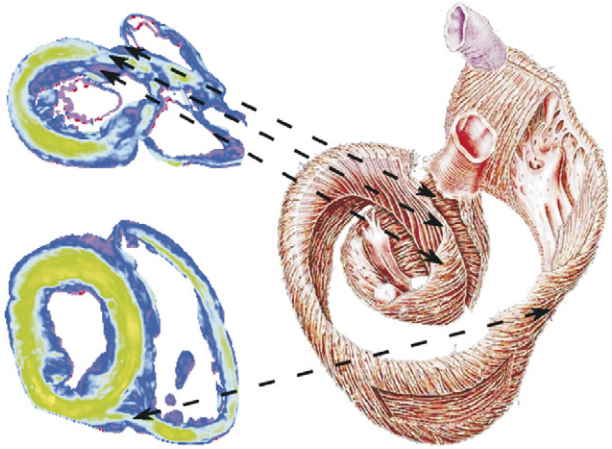

Fig. 8. Elevation maps of two coronal sections of the normal heart of a 10-week-old infant. The lower section is at the level of the papillary muscles of the left ventricle. There is continuity between the unrolled right ventricular free wall and the diaphragmatic face of the left ventricle, the basal loop. The upper section is on the left ventricular side 2 mm from the left atrioventricular junction, and on the right side at the level of the atrioventricular junction. In the subaortic region, there are sharp variations in fiber elevation inside and outside the circumferential fibers. Our data cannot confirm nor discard the existence of the apical loop of Torrent-Guasp's model. Double arrows have been plotted in order to tentatively establish correspondence between structures of Torrent-Guasp helical myocardial band (by courtesy of Pr Paul Lunkenheimer and IOS Press) and structures identified on elevation maps.

correspondences between the structures of the Torrent-Guasp's model and structures identified on elevation maps. During postnatal life, there is some continuity between the right ventricular free wall and the left ventricle, the basal loop. And it is possible to discern two muscular bands toward the outlet of the left ventricle on both sides of circumferential fibers. Numerical fiber tracking of these two bands somehow mimics the apical loop of Torrent-Guasp's model.

5. Discussion

Accuracies and limitations of quantitative polarized light analysis have been discussed from an experimental point of view. It has been possible to confirm with this technique on a larger scale Streeter's conjecture of fiber architecture of the left ventricle during fetal life. Meanwhile, we explained how to demonstrate from an experimental and mathematical point of view an hypothesis with the use of quantitative data. Then, we provided a new conjecture for the whole ventricular mass during fetal period. However, the validation of this conjecture remains to be done, although the insufficient definition of the elevation angle, the ambiguous fiber tracking and the absence of mathematical and numerical methods when there is no symmetry of revolution make it rather difficult. Besides, our data may be matched to other existing models. Clearly, Torrent-Guasp's model is not compatible with our data during the fetal period. However, after the major events of postnatal cardiovascular adaptation, our data cannot discard nor confirm Torrent-Guasp's model. This simple statement needs several explanations because there is a large difference in nature between our pretzel conjecture and Torrent-Guasp's conjecture. Our ambition is to display a simple geometrical description of the

arrangement of a three-dimensional array of orientation segments representing the mean direction of the myosin filaments in the ventricular mass. The ambition of Torrent-Guasp' conjecture is to highlight the existence in the ventricular mass of a reliable and reproducible way to dissect a myocardial band between the aorta and the pulmonary trunk, whatever the fiber orientation in this myocardial band that should be extremely heterogeneous. From our point of view, validation of Torrent-Guasp's conjecture amounts to the following problem: is it possible to identify inside the ventricular mass areas displaying a rapid variation of orientation between bundles of fibers? Unfortunately, as already said, the limitations of our technique make this verification impossible at the present moment. Presently, we are working on a tilting microscopical stage that will extend the definition range of the elevation angle to 180° and thus tackle the ambiguity of fiber tracking. Then, we will be able to experimentally and mathematically explore Torrent-Guasp's conjecture.

Acknowledgements

This work was supported by the Fonds National de la Science (ACI Modelisation mathématique, mécanique et numérique du Myocarde) and by the region Rhône-Alpes (Projet mathématiques pour ADéMo).

References

[1] Krehl L. Beiträge zur Kenntniss der Füllung und Entleerung des Herzens. Abh Math Phys Kl Saechs Akad Wiss 1891;17:341—62.
[2] Mall FP. On the muscular architecture of the ventricles of the human heart. Am J Anat 1911;11:211—66.
[3] Robb JS, Robb RC. The normal heart — anatomy and physiology of the structural units. Am Heart J 1942;23:455—67.
[4] Rushmer RF, Crystal DK, Wagner C. The functional anatomy of ventricular contraction. Circ Res 1953;1:162—70.
[5] Lev M, Simkins CS. Architecture of the human ventricular myocardium. Technique for study using a odification of the Mall—MacCallum method. Lab Invest 1956;5:396—409.
[6] Grant RP. Notes on the muscular architecture of the left ventricle. Circulation 1965;32:301—8.
[7] Torrent-Guasp F. Organizacion de la musculatura cardiaca ventricular. In: Zarco P, Perez J, editors. El Fallo mecànico del Corazon. Barcelona: Ediciones Toray; 1975. p. 3—36.
[8] Fernandez-Teran MA, Hurle JM. Myocardial fibre architecture of the human heart ventricles. Anat Rec 1982;204:137—47.
[9] Greenbaum RA, Ho SY, Gibson DG, Becker AE, Anderson RH. Left ventricular fibre architecture in man. Br Heart J 1981;45:248—63.
[10] Sanchez-Quintana D, Garcia-Martinez V, Hurle JM. Myocardial fibre architecture in the human heart. Anat Rec 1990;217:263—73.
[11] Hort W. Quantitative morphology and structural dynamics of the myocardium. Methods Achiev Exp Pathol 1971;5:3—21.
[12] Fox CC, Hutchins GM. The architecture of the human ventricular myocardium. Hopkins Med J 1972;130:289—99.
[13] Streeter Jr DD. Gross morphology and fibre geometry of the heart. In: Berne RM, Sperelakis N, Geiger SR, editors. Handbook of physiology. The cardiovascular system. Baltimore: Williams & Wilkins; 1979 . p. 61—112.
[14] Schmid P, Jaermann T, Boesiger P, Niederer PF, Lunkenheimer PP, Cryer CW, Anderson RH. Ventricular myocardial architecture as visualised in postmortem swine hearts using magnetic resonance diffusion tensor imaging. Eur J Cardiothorac Surg 2005;27:468—72.
[15] Usson Y, Parazza F, Jouk P-S, Michalowicz G. Method for the study of the three-dimensional orientation of myocardial cells by means of confocal scanning laser microscopy. J Microsc 1994;174:101—10.
[16] Press WH, Flannery B, Saul A, Teukolsky S, Vetterling W. Numerical recipes in C and C++. Integration of ordinary differential equations, the Runge—Kutta method, 2nd ed., Cambridge: Cambridge University Press; 2002.
[17] Mourad A, Biard L, Caillerie D, Jouk P-S, Raoult A, Usson Y. Geometrical modelling of the fibre organization in the human left ventricle. In: Proceedings of the first international workshop on functional imaging and modeling heart. Lecture Notes in Computer Science 2001, vol. 2230, pp. 32—8.
[18] Mourad A. Description topologique de l'architecture fibreuse et modélisation mécanique du myocarde, 9 décembre 2003. Thèse INPG.
[19] Jouk P-S, Usson Y, Michalowicz G, Grossi L. Three-dimensional cartography of the pattern of the myofibres in the second trimester fetal human heart. Anat Embryol 2000;202:103—18.